

CarbonVCA: A cadastral parcel-scale carbon emission forecasting framework for peak carbon emissions

Yao Yao^{a,b,1}, Zhenhui Sun^{c,1}, Linlong Li^d, Tao Cheng^e, Dongsheng Chen^{f,*}, Guangxiang Zhou^a, Chenxi Liu^g, Shihao Kou^a, Ziheng Chen^a, Qingfeng Guan^a

^a School of Geography and Information Engineering, China University of Geosciences, Wuhan 430078, Hubei Province, China

^b Center for Spatial Information Science, The University of Tokyo, Kashiwa-shi, Chiba 277-8568, Japan

^c Key Laboratory of Spatial-temporal Big Data Analysis and Application of Natural Resources in Megacities (Ministry of Natural Resources), School of Geographic Sciences, East China Normal University, Shanghai 200241, China

^d School of Resource and Environmental Science, Wuhan University, Wuhan 430079, Hubei Province, China

^e College of Surveying and Geo-Informatics, Tongji University, Shanghai 200092, China

^f Chair of Cartography and Visual Analytics, Technical University of Munich, Munich 80333, Germany

^g School of Computer Science, China University of Geosciences, Wuhan 430078, Hubei Province, China

ARTICLE INFO

Keywords:

Carbon emission forecasting
Vector-based cellular automata
Peak carbon emissions
Cadastral parcel
Urban ecology

ABSTRACT

Forecasting cities' carbon emissions is an essential support for peak carbon emissions. Previous studies have mainly focused on estimating carbon emissions at large regional scales. Higher spatial resolution mapping of carbon emissions and simulation of future scenarios are important to support locally appropriate policy guidance to reduce carbon emissions. This paper proposes a bottom-up cadastral parcel-scale Carbon emission forecasting framework based on Vector-based Cellular Automata (CarbonVCA) by integrating land use modelling and carbon emission estimation. Shenzhen's cadastral parcel-scale carbon emissions from 2020 to 2060 are predicted as a case study. A good performance was achieved using CarbonVCA (MAPE = 19.017 %, RMSE = 0.175 Mtpa (C)). Three progressive scenarios are designed for carbon emission simulation from land use planning and energy structure restructuring perspectives. The designed carbon emission reduction scenario limits carbon emissions and enables Shenzhen to achieve peak carbon emissions between 2025 and 2030. However, the efforts to reach peak carbon emissions may prompt the relocation of industrial land to the suburbs. Such areas will need appropriate infrastructure construction to break through terrain and landscape constraints, maintain economic growth and achieve sustainable development. This framework can forecast a high spatial resolution of land-use-based carbon emissions, which helps construct low-carbon cities.

1. Introduction

In recent years, global ecological problems, e.g., global warming and atmospheric pollution, have become a significant challenge for sustainable development. In September 2019, the United Nations Framework Convention on Climate Change stated that 60 countries worldwide have committed to reaching zero carbon emissions by 2050 (Iyer et al., 2017; Kuyper et al., 2018; Wamsler et al., 2020). Controlling carbon emissions has aroused widespread concern amongst nations worldwide (Akadiri et al., 2019). The Intergovernmental Panel on Climate Change

(IPCC) Special Report on Climate Change and Land state that the goal of keeping warming to well below 2 °C can only be achieved by reducing emissions from all industries (IPCC Technical Summary, 2019).

As the largest energy consumer (with an industrial output of US\$5.37 trillion), China emitted 10,313,460 kt of carbon in 2018, accounting for about 30 % of total global carbon emissions (Facts, 2009). At the 2014 Asia-Pacific Economic Cooperation (APEC) meeting, China pledged to peak its carbon emissions around 2030. Also, China has committed to reducing its CO₂ emissions per unit of GDP (Meng et al., 2020). However, China's carbon emissions are still increasing or plateauing as

* Corresponding author at: Technical University of Munich, Germany.

E-mail addresses: yaoy@cug.edu.cn, yaoy@csis.u-tokyo.ac.jp (Y. Yao), sunzhenhui@stu.ecnu.edu.cn (Z. Sun), lilinlong@whu.edu.cn (L. Li), chengtaoch@tongji.edu.cn (T. Cheng), dongsheng.chen@tum.de (D. Chen), zhougx9981@cug.edu.cn (G. Zhou), 20191001508@cug.edu.cn (C. Liu), 20151002461@cug.edu.cn (S. Kou), 3012857504@cug.edu.cn (Z. Chen), guanqf@cug.edu.cn (Q. Guan).

¹ These authors contributed equally to this work.

international energy-intensive industries, e.g., materials and manufacturing, continue shifting to Chinese cities (Yu et al., 2022). Hence, it is vital to evaluate China's urban carbon emissions for the goal of peak carbon emissions (Wang et al., 2018).

Forecasting cities' carbon emissions can effectively support governments in designing policies for reaching peak carbon emissions (Clark et al., 2016; Li et al., 2016). Some models were developed to assess carbon emission trends, including Logarithmic Mean Divisia Index (LMDI) model (Ding & Li, 2017), the Kaya model (Han et al., 2019), the Ideal Point Cross Efficiency (IPCE) model (Liu et al., 2018), and the Stochastic Impacts by Regression on Population, Affluence, and Technology model (Li & Lin, 2015). These models are usually based on data (e.g., population, energy consumption and demand) at large scales (e.g., the national and regional scale). Thus, they ignore the spatial heterogeneity of carbon emissions within the study region, resulting in a one-size-fits-all crude carbon emission management (Li et al., 2022; Liu, Guan, et al., 2015). Some models based on nighttime light data were also attempted to forecast carbon emission at a finer scale. However, the spatial resolution of their results is still limited by the low spatial resolution of the nighttime light data (1–10 km) (Guan et al., 2022; Lv & Liu, 2020). It is challenging to assist policymakers in drawing precise ecological red lines and developing policies tailored to local conditions (Wang et al., 2022). Thus, fine-scale prediction for carbon emission is essential for advanced precise carbon emission management.

Land use parcels can be a finer-scale unit for carbon emission estimations (Zhang et al., 2022). Land use dynamic, the spatio-temporal change of land use, is one of the critical factors affecting carbon emissions (Ma & Wang, 2015; Tao et al., 2013). Because the process of land use dynamic influences both the anthropogenic emissions and natural carbon sinks, leading to abrupt swings in the regional carbon cycle (Houghton & Nassikas, 2017; Zhu et al., 2019). Previous land-use dynamic-based models for predicting carbon emission can simulate high-spatiotemporal-resolution results of carbon emissions by using multi-source data integration (Dou et al., 2022), carbon emission coefficients (Zhou et al., 2021), or uncertainty in observation constraints (Lienert & Joos, 2018). They can provide a more detailed basis for urban carbon emissions management (Jia et al., 2020; Liu et al., 2019). However, two problems with these models constrain modern carbon management (Lai et al., 2016). On the one hand, they usually ignore the differences in carbon emissions between the various urban functions within the urban lands (Wang et al., 2022). On the other hand, they have limitations in effectively predicting the spatio-temporal distribution of future carbon emissions under diverse strategy scenarios (Li et al., 2022). A valid spatio-temporal simulation model for predicting future carbon emissions is not yet available, which is essential for urban planners to design more locally appropriate strategies for carbon emission management.

Land use dynamic can effectively be modelled via Geographical Cellular Automata (GeoCA) models (Batty, 1998; Clarke et al., 1997; Dahal & Chow, 2015; Li et al., 2017; Santé et al., 2010). Since real-world land-use parcels in urban planning are usually irregular polygons, vector-based land-use simulations are more reasonable and accurate (Lu et al., 2015). Thus, the emerging vector-based cellular automata (VCA) model can effectively reveal the relationship between various urban land-use types and the driving factors to achieve cadastral parcel-scale urban land use dynamic simulation (Yao et al., 2017; Yao et al., 2021). Moreover, the VCA models show the potential to explore the impact of policies on the spatio-temporal distribution of carbon emissions, thereby helping achieve peak carbon emissions following macro policy adjustments (Abolhasani et al., 2016; Yao et al., 2021; Zhai et al., 2020).

In summary, the current models for predicting urban carbon emissions show two deficiencies: the essential but neglected impact of urban land use dynamic on carbon emission changes (He et al., 2021) and the insufficiently high spatial resolution (Chuai et al., 2015). In addition, policymaker needs to understand the future trends in carbon emissions

from detailed urban land use dynamic under diverse strategy scenarios (Yao et al., 2021). Therefore, this paper proposes a bottom-up cadastral parcel-scale Carbon emission estimating and forecasting framework based on Vector-based Cellular Automata, namely CarbonVCA framework. Shenzhen, Guangdong Province, is taken as the study area. This framework integrates VCA models, a random forest classifier, and carbon emission coefficients for diverse land use types. It is designed to effectively model and analyse cadastral parcel-scale carbon emissions changes, contributing to the relevant policy guidance. The result is expected to help facilitate the rapid transformation of the economy and the development of ecologically conscious cities.

2. Study area and data

Shenzhen, Guangdong Province, is located in the Pearl River Delta region in south China (Fig. 1A). The city covers a total area of 1997.47 km², with nine administrative districts and one new district (Dapeng District) under its jurisdiction (Fig. 1B). Shenzhen is the fastest growing and large city as China's first special economic zone and one of the core cities in the Guangdong-Hong Kong-Macao Bay Area. In 2020, Shenzhen achieved a regional GDP of RMB 276,707,024 million and a resident population of 17.56 million (SSIB (Shenzhen Statistics and Information Bureau), 2010). However, its rapid urbanisation has brought about vast challenges of resource shortage and environmental pollution (Wang et al., 2010). Thus, Shenzhen urgently needs to enhance ecological and environmental management capabilities and achieve the city's peak carbon emissions and carbon-neutral targets.

Carbon emissions are strongly related to land use and dynamics (Ma & Wang, 2015; Tao et al., 2013). The probabilities of land-use transformation have to be calculated first to estimate the land-use-based carbon emissions. The cadastral land use data utilised here was obtained from the Shenzhen Municipal Bureau of Planning and Natural Resources (<https://pnr.sz.gov.cn/>) (Fig. 1C and D). The land use types include public service, residential, commercial, industrial, and unbuilt land.

The multi-source geographical data of topography, transportation, industrial, commercial, and residential facilities are used to calculate the spatial driving factors for the urban land use change (Table 1). The data pre-processing step is conducted to unify the data format to calculate the spatial driving factors. Here, all spatial variables are in the raster format. Then, kernel density analysis is used to transform the data in the Point Shapefile format to the corresponding spatial variables (Wand & Jones, 1994; Yuan et al., 2012). The data in the Line Shapefile format are converted to the corresponding spatial variables by calculating the Euclidean distances from all grids to the lines. Moreover, all the grid values are normalised to be between 0 and 1 with a spatial resolution of 30 m × 30 m (Fig. 2).

Statistics (such as land use percentage, residential building situation, distribution of public building types and electricity consumption) were selected to assist in the calculation of the land use-related carbon emission coefficients. These statistics were obtained from *Shenzhen Land Use Plan*, *Shenzhen Statistical Yearbook* and *Report on the Monitoring of Energy Consumption in Large Public Buildings in Shenzhen*. They are in text format containing Shenzhen's socioeconomic indicators. In addition, district-scale carbon emission inventories for Shenzhen from 2010 to 2017 are obtained to validate the carbon emissions accounted for in this paper (Chen, Gao, et al., 2020; Chen, Lu, et al., 2020). They are also in text format containing the annual figures for Shenzhen's carbon emissions.

3. Methodology

The framework includes four steps (Fig. 3). 1) Land-use type integration. This step aims to simplify the over-detailed and complex land use types. Similar land-use types are merged via a clustering algorithm. 2) Urban land use dynamic simulation. This step inputs the simplified

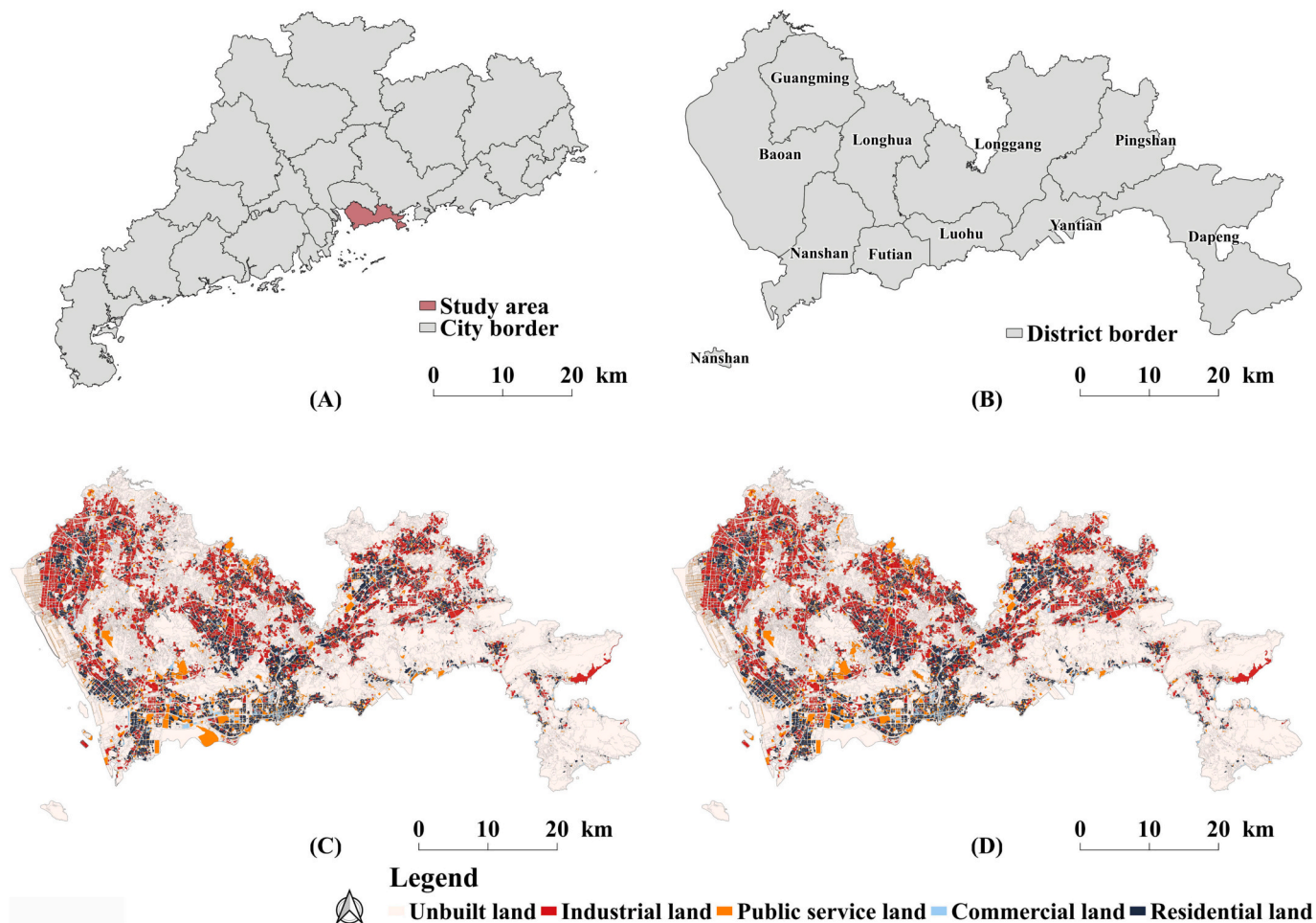


Fig. 1. Study area and the land use distributions. (A) Guangdong Province. (B) Shenzhen. (C) The cadastral land use data in 2009. (D) The cadastral land use data in 2014.

Table 1
Data sources of the multi-source geographical data.

Data	Format	Resolution	Data source	Year
DEM	GeoTiff	30 m	https://www.gscloud.cn/	/
Slope	GeoTiff	30 m	https://www.gscloud.cn/	/
OSM roads	Line	/	http://openstreetmap.org	/
Roads	Line	/	http://openstreetmap.org	/
Highways	Line	/	http://openstreetmap.org	/
Railways	Line	/	http://openstreetmap.org	/
Shopping facilities	Point	/	https://lbs.amap.com/	2018
Dining facilities	Point	/	https://lbs.amap.com/	2018
Recreational facilities	Point	/	https://lbs.amap.com/	2018
Medical facilities	Point	/	https://lbs.amap.com/	2018
Commercial facilities	Point	/	https://lbs.amap.com/	2018
Parklands	Point	/	https://lbs.amap.com/	2018
Bus facilities	Point	/	https://lbs.amap.com/	2018
Industrial facilities	Point	/	https://lbs.amap.com/	2018

land use data and the spatial variables into a VCA model to simulate the land use dynamic. 3) Land-use type decomposition. This step refines the simplified land-use types using the roulette strategy to estimate carbon emissions better. 4) Carbon emission forecasting. The cadastral parcel-scale carbon emissions are forecasted based on the simulated urban land use dynamic. And then, the spatio-temporal variations of carbon emissions are analysed under three scenarios to support urban carbon management decision-making.

3.1. Land use type integration

Land use type integration for a better VCA simulation was carried out for overall simulation accuracy improvement. The VCA models usually need to construct land use transformation rules through machine learning training (Yao et al., 2021). Over-detailed and complex land use types can reduce the simulation accuracy of VCA models for two reasons (Dietzel & Clarke, 2004). Firstly, the training sample size for each type is too small for the model to learn sufficiently (Ali et al., 2012). Secondly, it leads to over-complex land-use transformation rules, increasing the risk of misclassification (Ao et al., 2019). Hence, it is necessary to simplify the land use types.

The original land use types with similar landscape patterns are integrated into one simplified land use type. Landscape indices and a clustering algorithm are used to measure the similarity of their landscape patterns. Landscape indices can quantify the landscape pattern of the land parcels, e.g., size, shape, neighbourhood, texture, and diversity (Wang et al., 2019). Moreover, Yao et al. (2022) proposed vector-based

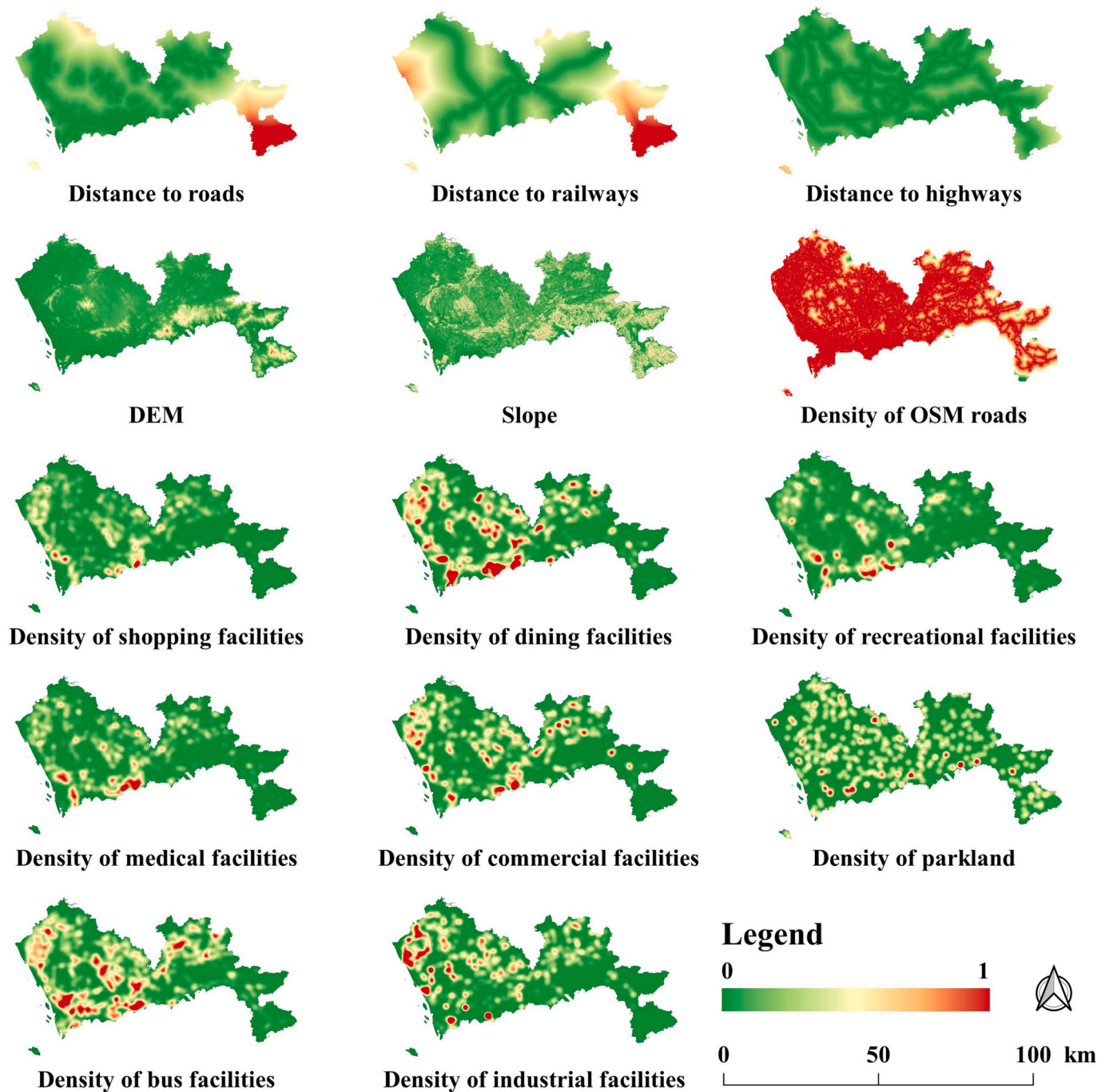


Fig. 2. Spatial driving factors calculated for the urban land use change.

landscape indices for vector-based land parcels to measure the vector-modified landscape patterns (Yao et al., 2022). Here, 17 metrics of vector-based landscape indices are applied to quantify the size, shape, diversity and agglomeration (Table S1).

The clustering algorithm combines original land-use types with similar landscape patterns (Ducret et al., 2016; Zheng et al., 2018). To verify the quality of the clustering result, Silhouette Coefficient is used as the accuracy metric. It effectively combines the cohesive and separating characteristics of clustering, thereby being widely used (Campello & Hruschka, 2006; Chen et al., 2014; Rousseeuw, 1987).

Given the number of clusters as n , Silhouette Coefficient is calculated as follows.

$$S_j = \frac{b_j - a_j}{\max\{a_j, b_j\}}$$

where S_j denotes the Silhouette Coefficient of vector j , a_j , b_j indicate the mean distance between vector j and all other vectors in the same cluster and the smallest mean distance of vector j to all vectors in any other cluster. The Silhouette Coefficient ranges from -1 to 1 . It indicates the best quality of clustering when it equals one.

3.2. Vector-based simulation of land-use dynamic

The crux of land-use dynamic modelling is to mine land-use transformation rules effectively. In our VCA model, the probability of land-

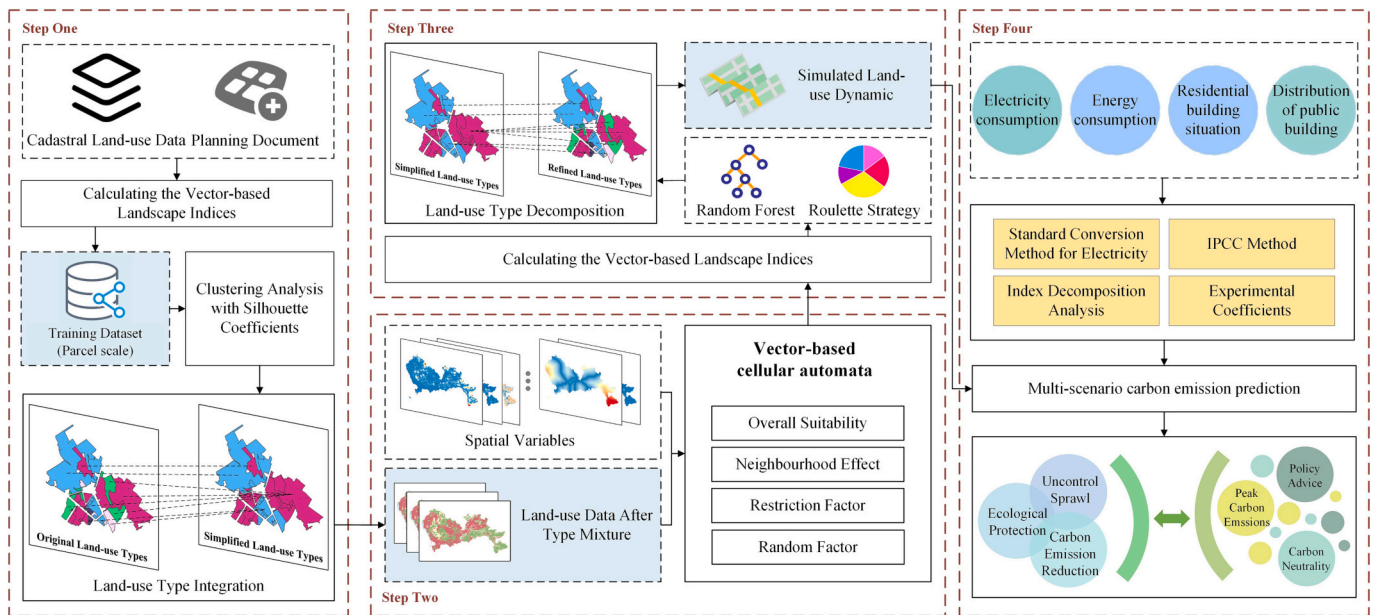


Fig. 3. Workflow of the proposed CarbonVCA framework.

use transformation consists of four components, i.e., the overall suitability P_g , the neighbourhood effect Ω , the restriction factor Pr , and the random factor RA . The probability for the i -th land parcel converting into the k -th type of land use at Moment t can be calculated as follows.

$$P_i^{k,t} = P_{g_i}^{k,t} \times \Omega_i^{k,t} \times Pr_i^t \times RA$$

In our VCA model, the land parcels are split based on a dichotomous strategy (Yao et al., 2017). The averages of the spatial variables for the split land-use parcels are defined as X . The probabilities of the transformed land-use types are defined as Y . And the model of $Y = f(X)$ can be constructed. Finally, the probability of the split parcel transforming into the land use type in the initial year Y_i is taken as the overall suitability of land-use transformation P_g .

The neighbourhood effect Ω is calculated based on the number and distribution of land use types within the set neighbourhood. This framework applies the neighbourhood radius to search for the centre of mass of land parcels to measure the neighbourhood effect for each land parcel (Abolhasani et al., 2016).

The restriction factor Pr simulates that the land use types cannot be transformed. Thus, Pr is set to 0 for development-restricted areas and 1 for suitable development areas. In addition, to simulate the uncertainty of the land-use transformation process, we introduced the random factor $RA = 1 + (-\ln y)^\alpha$, where α, y indicate a parameter ranging from 1 to 10 and a random value ranging from 0 to 1.

3.3. Land use type decomposition

The step of land use type decomposition is designed to obtain refined land use types from the simplified land use types for accurate carbon emission estimation. The refined land use types can improve the accuracy of carbon emission estimation (Liang, Guan, Clarke, Chen, et al., 2021; Liang, Guan, Clarke, Liu, et al., 2021). Because detailed land use types can establish clear, logical relationships with carbon emissions, which can determine more accurate carbon emission coefficients (Xu et al., 2019). Here, the possibility of decomposing each refined land use type from the specified simplified land use type is calculated using the random forest algorithm and the parcels' landscape indices. Define the means of the parcel landscape indices as X and the refined land use type as Y . Construct a $Y = f(X)$ model and take the probability of a parcel converting into each refined type Y_i as the probability of a parcel

actually being a certain refined category P_m .

The roulette strategy is applied to determine the final refined land use types based on the possibility obtained from the random forest algorithm (Liang, Guan, Clarke, Chen, et al., 2021; Liang, Guan, Clarke, Liu, et al., 2021) to simulate the uncertainty of the actual land use change. The advantage of this strategy is that it reserves the potential for refined land use types with a small probability (Luck & Wu, 2002). The details and the result of the land use type decomposition can be found in the section *Result of land use type integration and decomposition* in the Supplementary materials.

3.4. Carbon emission forecasting

This step aims to forecast the cadastral parcel-scale carbon emissions and analyse their spatio-temporal pattern based on the land use dynamic simulated in the above step. Two parts are included in this step. 1) Estimating carbon emission from urban land use. Different models are built to estimate carbon emissions depending on their corresponding land use types. 2) Multi-scenario carbon emission prediction. This study sets up three typical scenarios and predicts the corresponding future carbon emissions to tell what will happen and support urban development decision-making.

3.4.1. Estimating carbon emissions from urban land use

Here, different methods and models are applied to estimate carbon emissions depending on their corresponding land use types. Previous studies have proposed several widely-used methods for estimating carbon emission coefficients, e.g., the IPCC method (Amstel, 2015; Penman et al., 2006), the experimental measurement approach (Chen, Gao, et al., 2020; Chen, Lu, et al., 2020), and the adapted balance method (Schwarzböck et al., 2018). These methods show their different strengths in different situations. Firstly, the experimental measurement approach requires field measurements of emission sources, which is highly accurate but time-consuming. Thus, this approach is suitable for more stable land uses such as arable land, water bodies and forests. Here, we applied the experimental coefficients of carbon emissions for the above land use form (Chen, Gao, et al., 2020; Chen, Lu, et al., 2020). Secondly, the adapted balance method analyses the inputs and outputs of a production process, thereby being more applicable to industrial land use. Last, the IPCC method is one of the most used approaches of carbon estimation today, which can be used to estimate carbon emissions from

agricultural, forestry, energy, and industrial land uses. Here, we combine the above methods for different land uses to obtain a more reasonable result.

Regarding the built-up land use, its carbon is mainly emitted from power consumption (e.g., night lighting and air conditioning devices) (Shen et al., 2018). And the carbon emission coefficient for power consumption can be estimated via the standard coal conversion method for electricity. Thus, the carbon emission coefficient P_b for the built-up land use can be calculated as follows.

$$P_b = \sum \mu_k \cdot V \cdot T \quad (1)$$

where μ_k, V, T indicates the carbon emission coefficient for power consumption, power consumption per unit time of use in built-up areas, and duration of electricity use, respectively.

For industrial land use, its carbon emission coefficient P_i can be indirectly estimated via its energy consumption (Wang et al., 2016). Then, we can calculate Shenzhen's carbon emissions from industrial land use based on the IPCC method and energy consumption statistics (Xu et al., 2019).

Similarly, the following equation can obtain the carbon emission coefficients for public service, residential, and commercial land.

$$\delta = \frac{P}{S \times T} \quad (2)$$

where δ, P, T, S means the carbon emission coefficient for this type of land use, the carbon emissions from this type of land use, the duration of energy consumption and the total area, respectively.

The details of the reasoning process and the carbon emission coefficients for diverse land use types can be found in the section *Determination of carbon emission coefficients* in the Supplementary materials.

3.4.2. Multi-scenario carbon emission prediction

Three scenarios of simulating the urban development strategies are set to explore the impact of existing ecological protection policies on urban carbon emissions. (1) The uncontrolled sprawl scenario (Scenario I) indicates that all land use types can be transformed into each other. (2) The ecological protection scenario (Scenario II) means that the land parcels within ecological reserves are prohibited from being developed into built-up land to represent the application of the policy of ecological protection. And (3) the carbon emission reduction scenario (Scenario III) is designed in the context of the current land use planning policy. The carbon emission coefficients of industrial and commercial land use are designed to decay over time to simulate the contribution associated with emissions reduction policies, e.g., the structure adjustment for energy consumption. Here, similar to the previous VCA models, the future total land stock is predicted first by using the Markov Chain model. And then, our VCA model simulates the future land use dynamic based on the above scenarios and the future total land stock.

3.5. Accuracy assessment

Figure of Merit (FoM), Product's accuracy (PA) and User's accuracy (UA) are applied to assess the accuracy of the result of land-use dynamic simulation. Amongst, FoM is a standard metric in current cellular automata simulation research, which can comprehensively evaluate the performance of the model (Chen et al., 2014; Li, Li, et al., 2020; Li, Peoples, et al., 2020; Pontius et al., 2008). Previous studies suggested that a FoM of 0.2 or more represents a good simulation of the land use model. And the PA and UA generally indicate good model performance when they are between 0.2 and 0.4 (Yao et al., 2017; Zhai et al., 2020). Their equations are as follows.

$$FoM = B/(A + B + C + D) \quad (4)$$

$$PA = B/(A + B + C) \quad (5)$$

$$UA = B/(B + C + D) \quad (6)$$

where A, B, C, and D indicate the parcels that remain untransformed in simulation but have transformed in the ground truth, the parcels that correctly change land use as well as the correct changed land-use type, the parcels that correctly change land use but with a wrong changed land-use type, and the parcels that transform land use in simulation but remain untransformed in the ground truth, respectively.

To assess the error of the result of carbon emission measurement, we apply two metrics, i.e., root mean square error (RMSE) and mean absolute percentage error (MAPE). They are calculated at the county scale, as follows.

$$RMSE = \sqrt{\frac{1}{n} \sum_{i=1}^n (\hat{y}_i - y_i)^2} \quad (7)$$

$$MAPE = \frac{100\%}{n} \sum_{i=1}^n \left| \frac{\hat{y}_i - y_i}{y_i} \right| \quad (8)$$

where n, y_i, \hat{y}_i indicate the size of samples, the ground-truth carbon emission from the inventories, and the carbon emission estimated by the model, respectively.

4. Result

4.1. Simulation result of land-use dynamic

This paper simulates the land-use dynamic in Shenzhen from 2009 to 2014 using the VCA model. The model performs satisfactorily in most areas according to the criteria $FoM \geq 0.2$ (Table 2). The overall FoM in Shenzhen achieves 0.239. And the FoM in Longhua District, Guangming District and Baoan District even reach higher than 0.25, and their PA and UA are higher than 0.38. Moreover, the simulated result in 2014 is almost identical to the ground truth in 2014 (Fig. 4A and B). Hence, the simulation result of the land-use dynamic in Shenzhen is reasonable.

The correctly simulated land parcels are clustered in the northern part (Fig. 4C). It may be related to the fact that the northern part contains a lot of unbuilt-up land and has excellent potential for urbanisation. Thus, the proposed model can effectively tap into the land-use transformation patterns of emerging urban and distant suburban areas. This simulation result is conducive to exploring future urban land use development and improving the accuracy of urban carbon emission prediction. In addition, the reduction trend in the industrial land is simulated by the VCA model, revealing that some industrial land is being transformed in urban regeneration. Thus, the VCA model can provide a better insight into urban regeneration patterns, which has important implications for carbon emission modelling.

Table 2
Accuracy of the VCA-based land use simulation.

District	FoM	PA	UA
Nanshan	0.111	0.134	0.387
Luohu	0.214	0.376	0.327
Futian	0.169	0.389	0.230
Yantian	0.232	0.323	0.452
Dapeng	0.168	0.244	0.349
Pingshan	0.220	0.357	0.363
Longgang	0.244	0.444	0.349
Longhua	0.293	0.420	0.483
Baoan	0.254	0.384	0.420
Guangming	0.265	0.382	0.457
Shenzhen	0.239	0.370	0.399

The bold fonts represent the overall accuracy of all the above accuracies.

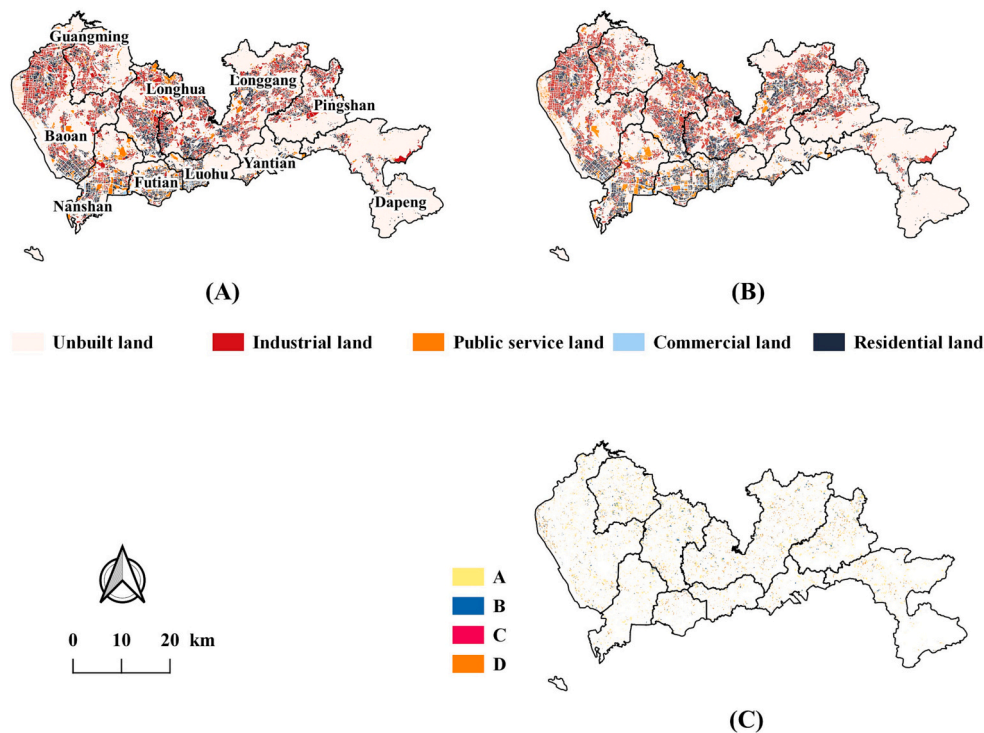


Fig. 4. Simulation result of the land-use dynamic. (A) Ground truth data in 2014. (B) Simulated result in 2014. (C) The correctly simulated and incorrectly simulated land parcels. A, B, C and D indicate the predicted land parcels in the four situations of FoM metric in Eq. (4).

4.2. Validation of the predicted carbon emissions

The predicted result and the ground truth at the district scale from 2015 to 2017 are compared (Table 3). Here, the predicted carbon emissions are aggregated to the 2010 version of the administrative district to keep them consistent with the ground truth since the current version is slightly different from the 2010 version. The predicted carbon emissions by the proposed model are consistent with the ground truth, presenting a high fitting accuracy (MAPE = 19.017 %, RMSE = 0.175 Mtpa (C)). Baoan District, Longgang District, Nanshan District and Luohu District achieved high fitting accuracy, while Futian District and Yantian District had average fitting accuracy.

Table 3
Comparison of predicted carbon emissions and ground truth data.

District	Year	Ground truth Mtpa (C)	Predicted result Mtpa (C)	MAPE	RMSE Mtpa (C)
Nanshan	2015	1.063	0.955	10.109 %	0.107
	2016	1.084	0.976	10.024 %	0.109
	2017	1.033	0.986	4.639 %	0.048
Luohu	2015	0.545	0.455	16.501 %	0.089
	2016	0.557	0.454	18.428 %	0.103
	2017	0.531	0.438	17.594 %	0.094
Futian	2015	0.456	0.589	29.299 %	0.134
	2016	0.465	0.593	27.508 %	0.128
	2017	0.443	0.590	33.380 %	0.148
Yantian	2015	0.410	0.137	66.628 %	0.273
	2016	0.430	0.164	61.794 %	0.266
	2017	0.419	0.169	59.663 %	0.250
Longgang	2015	3.466	3.421	1.268 %	0.044
	2016	3.556	3.521	0.973 %	0.034
	2017	3.407	3.561	4.525 %	0.154
Baoan	2015	3.849	4.236	10.059 %	0.387
	2016	3.926	4.267	8.675 %	0.341
	2017	3.725	4.228	13.859 %	0.502
Overall	2015	9.788	9.794	0.062 %	0.006
	2016	10.018	9.975	0.432 %	0.043
	2017	9.558	9.971	4.321 %	0.413

4.3. Spatio-temporal variation of Shenzhen's carbon emissions

Only Luohu District and Yantian District are estimated to reach peak carbon emissions by 2035 under Scenarios I and II in Shenzhen (Fig. 5). The carbon emissions from 2015 to 2060 are forecasted based on the future land use dynamic (Fig. S3). Although Scenario II can lead to more aggregation and a reduction in the cost of allocating urban resources, it cannot significantly reduce carbon emissions in the study area. Hence, the achievement of peak carbon emissions is dependent on the implementation of energy efficiency and emission reduction policies.

All districts in Shenzhen can achieve peak carbon emissions by around 2025 to 2030 under Scenario III. Currently, the annual rate of decline in carbon dioxide intensity per unit of energy consumption in China is about 1.2 % (Hu, 2021). If the development of Shenzhen's carbon structure continues to follow this trend in the future, combined with the share of fossil energy in Shenzhen, we define the annual decay rate of the carbon emission factor for industrial and commercial land in the carbon emission reduction scenario as 0.6 %. The carbon emission reduction scenario can lead to lower carbon emissions in all districts of Shenzhen than the other two scenarios. By around 2025 to 2030, Shenzhen's carbon emissions will change less, and the city will achieve peak carbon emissions. After 2030, Shenzhen's carbon emissions will decrease, with an annual rate of 0.211 %.

Futian District (Fig. 5b) and Luohu District (Fig. 5c) have shown a decreasing trend in carbon emissions since 2020. And Longgang District (Fig. 5d) is estimated to show a decreasing trend in carbon emissions since 2025. The carbon emissions of Baoan District (Fig. 5e), Nanshan District (Fig. 5g) and Longhua District (Fig. 5f) show a similar trend of slow increase and then decrease. And they will achieve the peak carbon emissions by 2025, 2026 and 2034, respectively. In Guangming District (Fig. 5i) and Pingshan District (Fig. 5h), carbon emissions stabilise after a short increase, and their peak carbon emissions will be reached by 2035 and 2030, respectively. In Yantian District (Fig. 5j), carbon emissions stabilise after a short period of shock, reaching a peak by 2037. The carbon emission of Dapeng District keeps oscillating over time. So it's

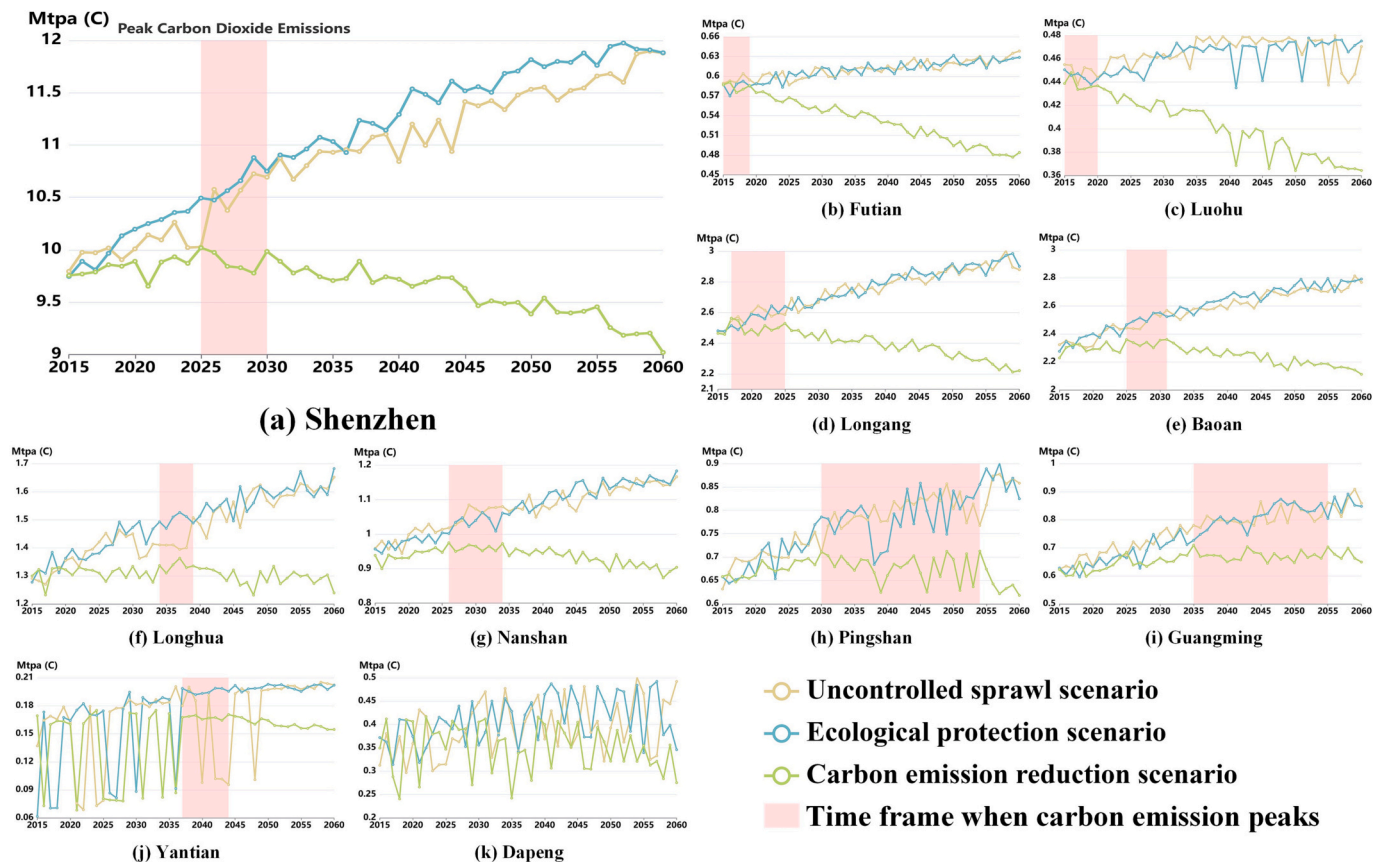


Fig. 5. Temporal trends of the forecasted carbon emissions under three strategy scenarios in Shenzhen.

impossible to estimate the exact time of achieving the peak carbon emissions.

The forecasted carbon emissions in 2060 in Shenzhen suggest that the efforts to reach peak carbon emissions may pose new challenges for infrastructure construction in suburban areas (Fig. 6A, B and C). The carbon emission of Pingshan District is much lower under the two controlled scenarios (the ecological protection scenario and the carbon emission reduction scenario) than that of the uncontrolled sprawl scenario. However, the northern part of Dapeng District shows higher carbon emissions under all the three scenarios. It may suggest that the two controlled scenarios will facilitate the relocation of industries from Pingshan District to Dapeng District, thereby resulting in a more concentrated distribution of industrial sectors. In addition, the temporal trends of the carbon emissions from 2015 to 2060 are further analysed (Fig. 6a, b and c). Firstly, the carbon emissions of industrial land vary most significantly in all scenarios, followed by unbuilt land. Secondly, the carbon emissions of all land types are the most stable in Scenario III. Even for industrial land, the range of variation is only around -0.15 to 0.15 . And for residential land, the carbon emissions remain stable over time, much lower than in Scenario I and II. The analysis is further discussed in the Discussion section.

5. Discussion

This paper proposes a bottom-up cadastral parcel-scale carbon emission estimating and forecasting framework, CarbonVCA, to help policymaking for urban carbon management. The proposed framework provides a new idea for urban carbon emission simulation from the land use perspective.

Shenzhen's future carbon emissions were forecasted and analysed. The simulation result shows a good performance, indicating the validity of the proposed framework. The overall MAPE for Shenzhen reached

1.605 %, and the average MAPE for each district reached 21.919 %. Specifically, the average MAPE in the coastal zone of Nanshan, the eastern part of Luohu and the central part of Longgang is 9.481 %. It indicates that the CarbonVCA framework is highly effective in modelling carbon emission changes in areas with high population concentration, high building density and high activity urban land development patterns (Guan et al., 2022; Lv & Liu, 2020). The conventional raster-based models for multi-scale carbon emission accounting usually rely on the high raster resolution at the finest scale. Thus, the raster resolution can easily lead to the accumulation of errors at large scales, such as the province and national scales (Liu et al., 2023). Compared to the raster-based models, CarbonVCA is no longer limited by the resolution. It can be used to investigate multi-scale carbon emissions without the negative impact of the accumulation of errors (Zhang et al., 2022).

Factors affecting the accuracy of the carbon emission simulations were explored and demonstrated via computer simulations to provide practical support for integrating urban land use modelling into carbon emission assessment. Firstly, the simulation accuracy is closely related to each district's total carbon emission. The lower the total carbon emissions of the district, the lower the simulation accuracy. And we notice that these regions with low carbon emissions are mainly covered by cultural land use, high-tech land use and finance-related land use. Their corresponding carbon emission coefficients are usually at low values, which may cause uncertainty in the step of land use type decomposition. Hence, these regions and their carbon coefficients may need to be further designed (Liu, Feng, et al., 2015; Liu, Guan, et al., 2015; Shan et al., 2018). For example, building census data and Gaode POI data will be integrated with other advanced algorithms further to improve the performance of the carbon emission modelling. Secondly, how the land uses evolve is affected by the future land stock predicted by the Markov Chain in the multi-scenario prediction. Specifically, when one land use type quickly reaches its land stock, the simulation process

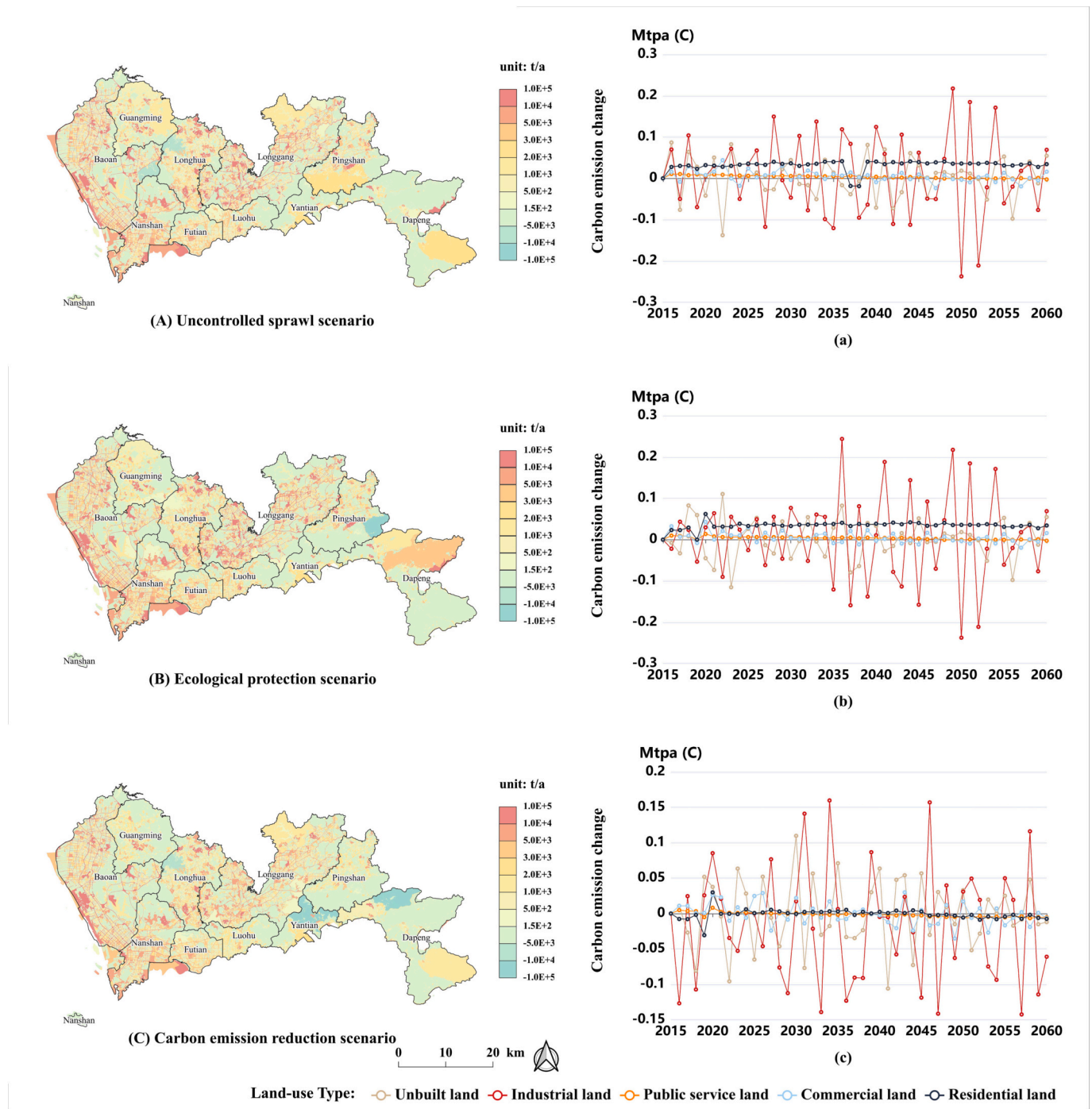


Fig. 6. Spatial distributions in 2060 (A, B and C) and temporal trends (a, b and c) of the forecasted carbon emissions under three strategy scenarios in Shenzhen.

will be locked up. Thus, the other land use types may not have enough time to evolve, which can affect the accuracy of carbon emissions predictions (Liang, Guan, Clarke, Chen, et al., 2021; Liang, Guan, Clarke, Liu, et al., 2021). In order to avoid this issue, the strategy of regional simulation will be applied to improve the accuracy further.

Our results have revealed distinct differences in the impact of three scenarios on future carbon emissions, which could be helpful for the government’s strategic decisions and policy making. Regarding the goal of peak carbon emissions, Scenarios I and II cannot significantly reduce the carbon emissions of Shenzhen. Because only two districts in Shenzhen, i.e., Luohu District and Yantian District, are estimated to achieve the goal around 2035 under these two scenarios. Hence, policy

interventions for carbon emission reduction are necessary. In addition, the carbon emissions of Futian District, Luohu District and Longgang District show a faster decline than those in other districts. Because essential administrative, cultural, financial and high-tech areas of Shenzhen are located in these districts, with advantages of a better ecological environment and a more liveable environment. In contrast, Yantian District and Dapeng District have experienced significant oscillations in their carbon emissions during the course of achieving peak carbon emissions, which is inextricably linked to their rapid development in recent years. The rapid urbanisation of Yantian District and Dapeng District in the future will lead to changes in the spatial distribution of land use. It will result in large oscillations in the carbon

emissions of the corresponding land parcels (Li, Li, et al., 2020; Li, Peoples, et al., 2020). In addition, this paper finds that under Scenario III, the carbon emissions of industrial land and unbuilt land change dramatically, while those of residential land and public service land change steadily. It suggests that the carbon emission reduction policy can ensure stable and green emissions from residential land and public service land, greatly alleviating the pressure on city carbon emissions. However, the carbon emission reduction policy intensifies the competition between industrial land and unbuilt land for land transformation (Tian et al., 2020). More attention is suggested to be paid to the scale and layout of future unbuilt land development. And the mixed-use mode of high-density land should be promoted to improve land use efficiency and realise the effective allocation and use of land resources (Bowley & Evins, 2020).

The results of this study can provide perspective and advice for Shenzhen's goal of achieving peak carbon emissions and carbon neutrality. Firstly, the results show that the Shenzhen government needs to adhere to an emissions reduction policy that combines land use planning with energy transition. China's average annual carbon emissions from anthropogenic sources are about 10 billion tonnes and are expected to reach 11 billion tonnes by 2030. Thus, the increase in carbon emissions must be controlled at 10 % (Xu et al., 2020; Yu et al., 2022). In the simulation scenario of ecological emissions reduction, Shenzhen's annual carbon emissions increased from 9.755 Mtpa (C) to 10.019 Mtpa (C), an increase of 2.706 %, in line with China's goal of peak carbon emission. Secondly, more attention should be paid to the future development of the Dapeng District and other suburban areas. Because the result shows that the land uses with high carbon emissions will shift from the Pingshan District to the Dapeng District. Previous studies have pointed out the existence of high-intensity industrial development in parts of the PingShan District and Dapeng District (Lai et al., 2020) and some potential hotspots for converting non-urban land to urban residential land (Zhuang et al., 2022). Constructing industrial land in Dapeng district is difficult due to its mountainous terrain, sloping land, low accessibility, and poor infrastructure. Hence, with its development limited by its environment and the ecological pilot, how to maintain its economic growth and achieve sustainable development is an issue that requires special attention in future policy formulation (Liang & Li, 2020). Our analysis also reminds the government that special attention needs to be paid to crucial national development areas to promote rapid economic and industrial transformation and achieve coordinated development in the context of sustainable development. While for the developed regions, the existing policies can be supplemented by demolishing and reconstructing some old facilities and optimising their layout to implement effective energy-saving and emission-reduction policies.

The proposed CarbonVCA model is an informative and intuitive tool to assist policymaking toward peak carbon emissions. To the best of our knowledge, the proposed CarbonVCA is the first model to incorporate differences in carbon emissions across various detailed urban land-use types. Carbon emissions from different urban functions are considered rationally to achieve accurate carbon emissions management. Secondly, the spatial heterogeneity of carbon emissions is portrayed at the cadastral parcel scale. In previous studies, carbon emission accounting was usually conducted on national, project, organisational, and product scales (Huo et al., 2022; Stechemesser & Guenther, 2012). The spatial resolution of their estimated carbon emissions is usually at the square kilometre scale (Yang & Li, 2022). Thus, it's difficult to precisely represent the spatial heterogeneity of carbon emissions within urban areas. This informative result can assist policymakers in drawing precise ecological red lines and avoiding the one-size-fits-all crude carbon emission management. Lastly, the future dynamic of carbon emissions can be predicted under diverse strategy scenarios. A significant advantage of the proposed CarbonVCA framework over existing models is that its intuitive results can directly estimate the potential impacts of various policies. It is essential to support the government in designing locally

appropriate guidelines for carbon emission management. Hence, we believe this convenient modelling tool can help cities take a further step toward the goal of peak carbon emissions.

Although the proposed model has generated accurate, informative and intuitive results of carbon emissions, our results need to be read with caution because of some deficiencies. Firstly, the step of land use type decomposition based on the machine learning algorithm is inevitably subject to some errors. Subsequent studies can couple multi-source data to investigate further the influence mechanism between landscape features and fine categories of land parcels. Secondly, the way of carbon emission estimation shows some limitations. The relationship between carbon emissions and electricity consumption within a specific land use type is complex and needs further exploration. Thus, our future research will address this issue via field surveys and more advanced methods. Finally, reducing carbon emissions in cities is related to using green energy and education to improve residents' habits of low-carbon consumption. In the future, more scenarios can be designed to provide more references for urban emissions reduction policies.

6. Conclusion

This paper proposes CarbonVCA, a bottom-top framework, for forecasting cadastral parcel-scale carbon emissions. This framework can effectively improve the spatial resolution of carbon emission forecasting. The framework achieves good accuracy in carbon emission modelling and provides practical support for integrating urban land use modelling into carbon emission assessment. The simulation result suggests that the government pays more attention to combining land use planning with energy transition and increasing infrastructure in the suburbs to peak carbon emission and carbon neutrality on schedule. This study can provide a reference for the regional setting of carbon emission allowances and promote the construction of a green and low-carbon city. In the future, this research will consider the development patterns of more cities, build a large-scale refined carbon emission prediction platform, accurately assess the carbon emission characteristics of different industrial land uses and analyse their impact mechanisms. So the result can help optimise the spatial structure of cities and thus construct ecologically oriented cities.

CRedit authorship contribution statement

Yao Yao: Conceptualization, Formal analysis, Writing – review & editing, Funding acquisition. **Zhenhui Sun:** Methodology, Validation, Formal analysis, Writing – original draft. **Linlong Li:** Methodology, Software, Validation, Data curation. **Tao Cheng:** Methodology, Investigation, Visualization, Data curation. **Dongsheng Chen:** Formal analysis, Writing – review & editing, Supervision. **Guangxiang Zhou:** Investigation. **Chenxi Liu:** Validation. **Shihao Kou:** Visualization. **Ziheng Chen:** Data curation. **Qingfeng Guan:** Writing – review & editing, Project administration, Funding acquisition.

Declaration of interest statement

No conflict of interest exists in the submission of this manuscript, and manuscript is approved by all authors for publication. I would like to declare on behalf of my co-authors that the work described was original research that has not been published previously, and not under consideration for publication elsewhere, in whole or in part.

Data availability

The figures with a high resolution supporting the present study's findings are available on Figshare at <https://figshare.com/s/fe7c507755c9350dbf12>.

Acknowledgements

This work was supported by the National Key Research and Development Program of China [2019YFB2102903], the National Natural Science Foundation of China [41801306, 41671408]; the “CUG Scholar” Scientific Research Funds at China University of Geosciences (Wuhan) [2022034] and a grant from State Key Laboratory of Resources and Environmental Information System; Alibaba Group through Alibaba Innovation Research Program [20228670]; China Scholarship Council [202208440090].

Appendix A. Supplementary data

Supplementary data to this article can be found online at <https://doi.org/10.1016/j.cities.2023.104354>.

References

- Abolhasani, S., Taleai, M., Karimi, M., & Rezaee Node, A. (2016). Simulating urban growth under planning policies through parcel-based cellular automata (ParCA) model. *International Journal of Geographical Information Science*, 30(11), 2276–2301.
- Akadiri, S. S., Bekun, F. V., Taheri, E., & Akadiri, A. C. (2019). Carbon emissions, energy consumption and economic growth: A causality evidence. *International Journal of Energy Technology and Policy*, 15(2–3), 320–336.
- Ali, J., Khan, R., Ahmad, N., & Maqsood, I. (2012). Random forests and decision trees. *International Journal of Computer Science Issues*, 9(5), 272–278.
- Amstel, A. V. (2015). *IPCC 2006 guidelines for national greenhouse gas inventories (issue November)*. IPCC 2006 guidelines for national greenhouse gas inventories.
- Ao, Y., Li, H., Zhu, L., Ali, S., & Yang, Z. (2019). Identifying channel sand-body from multiple seismic attributes with an improved random forest algorithm. *Journal of Petroleum Science and Engineering*, 173, 781–792.
- Batty, M. (1998). Urban evolution on the desktop: Simulation with the use of extended cellular automata. *Environment & Planning A*, 30(11), 1943–1967.
- Bowley, W., & Ewins, R. (2020). Assessing energy and emissions savings for space conditioning, materials and transportation for a high-density mixed-use building. *Journal of Building Engineering*, 31, Article 101386.
- Campello, R. J. G. B., & Hruschka, E. R. (2006). A fuzzy extension of the silhouette width criterion for cluster analysis. *Fuzzy Sets and Systems*, 157(21), 2858–2875.
- Chen, J., Gao, M., Cheng, S., Hou, W., Song, M., Liu, X., Liu, Y., & Shan, Y. (2020). County-level CO₂ emissions and sequestration in China during 1997–2017. *Scientific Data*, 7(1), 1–12.
- Chen, Y., Li, X., Liu, X., & Ai, B. (2014). Modeling urban land-use dynamics in a fast developing city using the modified logistic cellular automaton with a patch-based simulation strategy. *International Journal of Geographical Information Science*, 28(2), 234–255.
- Chen, Y., Lu, H., Li, J., & Xia, J. (2020). Effects of land use cover change on carbon emissions and ecosystem services in Chengyu urban agglomeration, China. *Stochastic Environmental Research and Risk Assessment*, 34(8), 1197–1215.
- Chu, X., Huang, X., Wang, W., Zhao, R., Zhang, M., & Wu, C. (2015). Land use, total carbon emissions change and low carbon land management in Coastal Jiangsu, China. *Journal of Cleaner Production*, 103, 77–86.
- Clark, P. U., Shakun, J. D., Marcott, S. A., Mix, A. C., Eby, M., Kulp, S., Levermann, A., Milne, G. A., Pfister, P. L., Santer, D. P., Schrag, D. P., Solomon, S., Stocker, T. F., Strauss, B. H., Weaver, A. J., Winkelmann, R., Archer, D., Bard, E., Goldner, A., Plattner, G. K., ... (2016). Consequences of twenty-first-century policy for multi-millennial climate and sea-level change. *Nature Climate Change*, 6(4), 360–369.
- Clarke, K. C., Hoppen, S., & Gaydos, L. (1997). A self-modifying cellular automaton model of historical urbanisation in the San Francisco Bay area. *Environment and Planning B: Planning & Design*, 24(2), 247–261.
- Dahal, K. R., & Chow, T. E. (2015). Characterisation of neighborhood sensitivity of an irregular cellular automata model of urban growth. *International Journal of Geographical Information Science*, 29(3), 475–497.
- Dietzel, C., & Clarke, K. C. (2004). Replication of spatio-temporal land use patterns at three levels of aggregation by an urban cellular automata. *Lecture Notes in Computer Science*, 3305, 523–532.
- Ding, Y., & Li, F. (2017). In 125. *Examining the effects of urbanisation and industrialisation on carbon dioxide emission: Evidence from China's provincial regions* (pp. 533–542).
- Dou, X., Wang, Y., Ciais, P., Chevallier, F., Davis, S. J., Crippa, M., Janssens-Maenhout, G., Guizzardi, D., Solazzo, E., Yan, F., Huo, D., Zheng, B., Zhu, B., Cui, D., Ke, P., Sun, T., Wang, H., Zhang, Q., Gentile, P., Liu, Z., ... (2022). Near-real-time global gridded daily CO₂ emissions. *Innovations*, 3(1), Article 100182.
- Ducret, R., Lemarié, B., & Roset, A. (2016). Cluster analysis and spatial modeling for urban freight. Identifying homogeneous urban zones based on urban form and logistics characteristics. *Transportation Research Procedia*, 12, 301–313.
- Facts, C. (2009). GHG emissions. 1–2. <http://www.epa.gov/greeningepa/ghg/>.
- Guan, W., Li, S., & Xu, S. (2022). Multiscale spatio-temporal characteristics of carbon emissions in Northeast China based on DMSP/OLS nighttime light data. *Ecological Economics*, 11(38), 19–26.
- Han, X., Cao, T., & Sun, T. (2019). Analysis on the variation rule and influencing factors of energy consumption carbon emission intensity in China's urbanisation construction. *Journal of Cleaner Production*, 238, Article 117958.
- He, H., Zhao, Y., & Wu, J. (2021). Simulation of urban landscape pattern under the influence of low carbon: A case study of Shenzhen. *Acta Ecologica Sinica*, 41(21), 8352–8363.
- Houghton, R. A., & Nassikas, A. A. (2017). Global and regional fluxes of carbon from land use and land cover change 1850–2015. *Global Biogeochemical Cycles*, 31(3), 456–472.
- Hu, A. (2021). China's goal of achieving carbon peak by 2030 and its main approaches. *Journal of Beijing Institute of Technology*, 21(3), 1–15.
- Huo, D., Huang, X., Dou, X., Ciais, P., Li, Y., Deng, Z., Wang, Y., Cui, D., Benkhelifa, F., Sun, T., Zhu, B., Roest, G., Gurney, K. R., Ke, P., Guo, R., Lu, C., Lin, X., Lovell, A., Appleby, K., Liu, Z., ... (2022). Carbon monitor cities near-real-time daily estimates of CO₂ emissions from 1500 cities worldwide. *Scientific Data*, 9(1), 533.
- IPCC Technical Summary. (2019). Foreword technical and preface, climate change and land: An IPCC special report on climate change, desertification, land degradation, sustainable land management, food security, and greenhouse gas fluxes in terrestrial ecosystems. In *Climate change and land: An IPCC special report on climate change, desertification, land degradation, sustainable land management, food security, and greenhouse gas fluxes in terrestrial ecosystems (Issues vii, 973)*. <https://www.ipcc.ch/srcl/download/>.
- Iyer, G., Ledna, C., Clarke, L., Edmonds, J., McJeon, H., Kyle, P., & Williams, J. H. (2017). Measuring progress from nationally determined contributions to mid-century strategies. *Nature Climate Change*, 7(12), 871–874.
- Jia, T., Yang, S., Li, X., Yan, P., Yu, X., Luo, X., & Chen, K. (2020). Computation of carbon emissions of residential buildings in Wuhan and its spatiotemporal analysis. *Journal of Geo-Information Science*, 22(5), 1063–1072.
- Kuyper, J., Schroeder, H., & Linnér, B. O. (2018). The evolution of the UNFCCC. *Annual Review of Environment and Resources*, 43(1), 343–368.
- Lai, L., Huang, X., Yang, H., Chuai, X., Zhang, M., Zhong, T., Chen, Z., Chen, Y., Wang, X., & Thompson, J. R. (2016). Carbon emissions from land-use change and management in China between 1990 and 2010. *Science Advances*, 2(11), Article e1601063.
- Lai, Y., Chen, K., Zhang, J., & Liu, F. (2020). *Transformation of industrial land in urban renewal in Shenzhen, China*. 9(10).
- Li, B., Gasser, T., Ciais, P., Piao, S., Tao, S., Balkanski, Y., Hauglustaine, D., Boisier, J. P., Chen, Z., Huang, M., Zhaoxin Li, L., Li, Y., Liu, H., Liu, J., Peng, S., Shen, Z., Sun, Z., Wang, R., Wang, T., Zhou, F., ... (2016). The contribution of China's emissions to global climate forcing. *Nature*, 531(7594), 357–361.
- Li, F., Li, Z., Chen, H., Chen, Z., & Li, M. (2020). An agent-based learning-embedded model (ABM-learning) for urban land use planning: A case study of residential land growth simulation in Shenzhen, China. *Land Use Policy*, 95, Article 104620.
- Li, K., & Lin, B. (2015). Impacts of urbanisation and industrialisation on energy consumption/CO₂ emissions: Does the level of development matter? *Renewable and Sustainable Energy Reviews*, 52, 1107–1122.
- Li, X., Chen, Y., Liu, X., Xu, X., & Chen, G. (2017). Experiences and issues of using cellular automata for assisting urban and regional planning in China. *International Journal of Geographical Information Science*, 31(8), 1606–1629.
- Li, X., Peoples, J., Huang, Z., Zhao, Z., Qiu, J., & Ruan, X. (2020). Full daytime sub-ambient radiative cooling in commercial-like paints with high figure of merit. *Cell Reports Physical Science*, 1(10), Article 100221.
- Li, Z., Wang, F., Kang, T., Wang, C., Chen, X., Miao, Z., Zhang, L., Ye, Y., & Zhang, H. (2022). Exploring differentiated impacts of socioeconomic factors and urban forms on city-level CO₂ emissions in China: Spatial heterogeneity and varying importance levels. *Sustainable Cities and Society*, 84, Article 104028.
- Liang, J., & Li, Y. (2020). Resilience and sustainable development goals based social-ecological indicators and assessment of coastal urban areas — A case study of Dapeng New District, Shenzhen, China. *Watershed Ecology and the Environment*, 2, 6–15.
- Liang, X., Guan, Q., Clarke, K. C., Chen, G., Guo, S., & Yao, Y. (2021). Mixed-cell cellular automata: A new approach for simulating the spatio-temporal dynamics of mixed land use structures. *Landscape and Urban Planning*, 205, Article 103960.
- Liang, X., Guan, Q., Clarke, K. C., Liu, S., Wang, B., & Yao, Y. (2021). Understanding the drivers of sustainable land expansion using a patch-generating land use simulation (PLUS) model: A case study in Wuhan, China. *Computers, Environment and Urban Systems*, 85, Article 101569.
- Lienert, S., & Joos, F. (2018). In 15(9). *A Bayesian ensemble data assimilation to constrain model parameters and land-use carbon emissions* (pp. 2909–2930).
- Liu, B., Tian, C., Li, Y., Song, H., & Ma, Z. (2018). Research on the effects of urbanisation on carbon emissions efficiency of urban agglomerations in China. *Journal of Cleaner Production*, 197, 1374–1381.
- Liu, X., Jin, X., Luo, X., & Zhou, Y. (2023). Multi-scale variations and impact factors of carbon emission intensity in China. *The Science of the Total Environment*, 857, Article 159403.
- Liu, Y., Hu, X., Wu, H., Zhang, A., Feng, J., & Gong, J. (2019). Spatiotemporal analysis of carbon emissions and carbon storage using national geography census data in Wuhan, China. *ISPRS International Journal of Geo-Information*, 8(1), 7.
- Liu, Z., Feng, K., Hubacek, K., Liang, S., Anadon, L. D., Zhang, C., & Guan, D. (2015). Four system boundaries for carbon accounts. *Ecological Modelling*, 318, 118–125.
- Liu, Z., Guan, D., Wei, W., Davis, S. J., Ciais, P., Bai, J., Peng, S., Zhang, Q., Hubacek, K., Marland, G., Andres, R. J., Crawford-Brown, D., Lin, J., Zhao, H., Hong, C., Boden, T. A., Feng, K., Peters, G. P., Xi, F., He, K., ... (2015). Reduced carbon emission estimates from fossil fuel combustion and cement production in China. *Nature*, 524(7565), 335–338.
- Lu, Y., Cao, M., & Zhang, L. (2015). A vector-based cellular automata model for simulating urban land use change. *Chinese Geographical Science*, 25(1), 74–84.
- Luck, M., & Wu, J. (2002). A gradient analysis of urban landscape pattern: A case study from the Phoenix metropolitan region, Arizona, USA. *Landscape Ecology*, 17(4), 327–339.

- Lv, Q., & Liu, H. B. (2020). In *40. Multiscale spatio-temporal characteristics of carbon emission of energy consumption in Yellow River basin based on the nighttime light datasets* (pp. 12–21).
- Ma, X., & Wang, Z. (2015). Progress in the study on the impact of land-use change on regional carbon sources and sinks. *Acta Ecologica Sinica*, *35*(17), 5898–5907.
- Meng, M., Shang, W., Wang, X., & Pang, T. (2020). When will China fulfill its carbon-related intended nationally determined contributions? An in-depth environmental Kuznets curve analysis. *Greenhouse Gases: Science and Technology*, *10*(5), 1039–1049.
- Penman, J., Gytarsky, M., Hiraishi, T., Irving, W., & Krug, T. (2006). 2006 IPCC - guidelines for national greenhouse gas inventories. directrices para los inventar. *Nac. GEI*, *12*. <http://www.ipcc-nggip.iges.or.jp/public/2006gl/index.html>.
- Pontius, R. G., Boersma, W., Castella, J. C., Clarke, K., Nijs, T., Dietzel, C., Duan, Z., Fotsing, E., Goldstein, N., Kok, K., Koomen, E., Lippitt, C. D., McConnell, W., Mohd Sood, A., Pijanowski, B., Pithadia, S., Sweeney, S., Trung, T. N., Veldkamp, A. T., & Verburg, P. H. (2008). Comparing the input, output, and validation maps for several models of land change. *The Annals of Regional Science*, *42*(1), 11–37.
- Rousseeuw, P. J. (1987). Silhouettes: A graphical aid to the interpretation and validation of cluster analysis. *Journal of Computational and Applied Mathematics*, *20*(C), 53–65.
- Santé, I., García, A. M., Miranda, D., & Crecente, R. (2010). Cellular automata models for the simulation of real-world urban processes: A review and analysis. *Landscape and Urban Planning*, *96*(2), 108–122.
- Schwarzböck, T., Aschenbrenner, P., Spacek, S., Szidat, S., Rechberger, H., & Fellner, J. (2018). In *220. An alternative method to determine the share of fossil carbon in solid refuse-derived fuels – Validation and comparison with three standardised methods* (pp. 916–930).
- Shan, Y., Guan, D., Hubacek, K., Zheng, B., Davis, S. J., Jia, L., Liu, J., Liu, Z., Fromer, N., Mi, Z., Meng, J., Deng, X., Li, Y., Lin, J., Schroeder, H., Weisz, H., & Schellnhuber, H. J. (2018). City-level climate change mitigation in China. *Science Advances*, *4*(6), Article eaaq0390.
- Shen, L., Wu, Y., Lou, Y., Zeng, D., Shuai, C., & Song, X. (2018). What drives the carbon emission in the chinese cities?—A case of pilot low carbon city of Beijing. *Journal of Cleaner Production*, *174*, 343–354.
- SSIB (Shenzhen Statistics and Information Bureau). (2010). *Shenzhen statistical yearbook 2010*. Beijing, China: China Statistics Press.
- Stechemesser, K., & Guenther, E. (2012). Carbon accounting: A systematic literature review. *Journal of Cleaner Production*, *36*, 17–38.
- Tao, B., Tian, H., Chen, G., Ren, W., Lu, C., Alley, K. D., Xu, X., Liu, M., Pan, S., & Virji, H. (2013). Terrestrial carbon balance in tropical Asia: Contribution from cropland expansion and land management. *Global and Planetary Change*, *100*, 85–98.
- Tian, J., Wang, B., Zhang, C., Li, W., & Wang, S. (2020). Mechanism of regional land use transition in underdeveloped areas of China: A case study of Northeast China. *Land Use Policy*, *94*, Article 104538.
- Wamsler, C., Schöpke, N., Fraude, C., Stasiak, D., Bruhn, T., Lawrence, M., Schroeder, H., & Mundaca, L. (2020). Enabling new mindsets and transformative skills for negotiating and activating climate action: Lessons from UNFCCC conferences of the parties. *Environmental Science & Policy*, *112*, 227–235.
- Wand, M. P., & Jones, M. C. (1994). Multivariate plug-in bandwidth selection. *Computational Statistics*, *9*(2), 97–116.
- Wang, C. C., Lin, G. C. S., & Li, G. (2010). Industrial clustering and technological innovation in China: New evidence from the ICT industry in Shenzhen. *Environment & Planning A*, *42*(8), 1987–2010.
- Wang, G., Han, Q., & de Vries, B. (2019). Assessment of the relation between land use and carbon emission in Eindhoven, the Netherlands. *Journal of Environmental Management*, *247*, 413–424.
- Wang, M., Wang, Y., Wu, Y., Yue, X., Wang, M., & Hu, P. (2022). Identifying the spatial heterogeneity in the effects of the construction land scale on carbon emissions: Case study of the Yangtze River Economic Belt, China. *Environmental Research*, *212*, Article 113397.
- Wang, Q., Wang, D., Yan, X., & Su, Q. (2016). An analysis on carbon emission effects in Yantai City based on decoupling theory. *Bulletin of Soil and Water Conservation*, *35*(2), 313–318.
- Wang, Y., Cheng, Y., Yang, G. C., & Dong, Y. (2018). Provincial decomposition of China's carbon emission rights under the constraint of 2020 and 2030 carbon intensity targets. *Zhongguo Huanjing Kexue*, *38*(8), 3180–3188.
- Xu, G., Schwarz, P., & Yang, H. (2020). Adjusting energy consumption structure to achieve China's CO2 emissions peak. *Renewable and Sustainable Energy Reviews*, *122*, Article 109737.
- Xu, J., Pan, H., & Huang, P. (2019). Carbon emission and ecological compensation of main functional areas in Sichuan Province based on LUCC. *Chinese Journal of Eco-Agriculture*, *27*(1), 142–152.
- Yang, Y., & Li, H. (2022). Monitoring spatiotemporal characteristics of land-use carbon emissions and their driving mechanisms in the Yellow River Delta: A grid-scale analysis. *Environmental Research*, *214*, 114151.
- Yao, Y., Cheng, T., Sun, Z., Li, L., Chen, D., Chen, Z., Wei, J., & Guan, Q. (2022). VecLI: A framework for calculating vector landscape indices considering landscape fragmentation. *Environmental Modelling and Software*, *149*, Article 105325.
- Yao, Y., Li, L., Liang, Z., Cheng, T., Sun, Z., Luo, P., Guan, Q., Zhai, Y., Kou, S., Cai, Y., Li, L., Ye, X., & Kong, H. (2021). UrbanVCA: A vector-based cellular automata framework to simulate the urban land-use change at the land-parcel level.
- Yao, Y., Liu, X., Li, X., Liu, P., Hong, Y., Zhang, Y., & Mai, K. (2017). Simulating urban land-use changes at a large scale by integrating dynamic land parcel subdivision and vector-based cellular automata. *International Journal of Geographical Information Science*, *31*(12), 2452–2479.
- Yu, G., Hao, T., & Zhu, J. (2022). Discussion on action strategies of China's carbon peak and carbon neutrality. *Bulletin of the Chinese Academy of Sciences*, *37*(4), 423–434.
- Yuan, J., Zheng, Y., & Xie, X. (2012). Discovering regions of different functions in a city using human mobility and POIs. In *Proc. ACM SIGKDD int. conf. knowl. discov. data min* (pp. 186–194).
- Zhai, Y., Yao, Y., Guan, Q., Liang, X., Li, X., Pan, Y., Yue, H., Yuan, Z., & Zhou, J. (2020). Simulating urban land use change by integrating a convolutional neural network with vector-based cellular automata. *International Journal of Geographical Information Science*, *34*(7), 1475–1499.
- Zhang, C., Zhao, L., Zhang, H., Chen, M., Fang, R., Yao, Y., Zhang, Q., & Wang, Q. (2022). Spatial-temporal characteristics of carbon emissions from land use change in Yellow River Delta region, China. *Ecological Indicators*, *136*, Article 108623.
- Zheng, Z., Du, S., Wang, Y. C., & Wang, Q. (2018). Mining the regularity of landscape-structure heterogeneity to improve urban land-cover mapping. *Remote Sensing of Environment*, *214*, 14–32.
- Zhou, Y., Chen, M., Tang, Z., & Mei, Z. (2021). Urbanisation, land use change, and carbon emissions: Quantitative assessments for city-level carbon emissions in Beijing-Tianjin-Hebei region. *Sustainable Cities and Society*, *66*, Article 102701.
- Zhu, E., Deng, J., Zhou, M., Gan, M., Jiang, R., Wang, K., & Shahtahmassebi, A. R. (2019). Carbon emissions induced by land-use and land-cover change from 1970 to 2010 in Zhejiang, China. *The Science of the Total Environment*, *646*, 930–939.
- Zhuang, H., Liu, X., Yan, Y., Zhang, D., He, J., He, J., Zhang, X., Zhang, H., & Li, M. (2022). Integrating a deep forest algorithm with vector-based cellular automata for urban land change simulation. *Transactions in GIS*, *26*(4), 2056–2080.